Electrochimica Acta 54 (2009) 5216–5222

Contents lists available at ScienceDirect

Electrochimica Acta

journal homepage: www.elsevier.com/locate/electacta

Steel corrosion in alkaline batteries

I. Serebrennikova [a], I. Paramasivam [b], P. Roy [b], W. Wei [b], S. Virtanen [b], P. Schmuki [b,*]

[a] Energizer Battery Co., 25225 Detroit Road, Westlake, OH 44145, USA
[b] Department of Materials Science, WW4-LKO, University of Erlangen-Nuremberg, Martensstrasse 7, D-91058 Erlangen, Germany

ARTICLE INFO

Article history:
Received 15 November 2008
Received in revised form 1 February 2009
Accepted 6 February 2009
Available online 14 February 2009

Keywords:
Steel
Corrosion
Alkaline batteries

ABSTRACT

During extended shelf storage and accelerated aging, low carbon steel may corrode producing soluble iron species that cause internal cell shorting and/or gassing (leakage), thus undermining battery reliability. Soluble iron may be generated from the active/passive and/or transpassive dissolution of the battery can steel. To minimize corrosion effects in commercial battery applications, NiCo plated steel is typically used. This report focuses on corrosion behavior of pure metals (iron, nickel, and cobalt) in 40% KOH at temperatures between 20 °C and 80 °C. A marked difference is found for the elements regarding the actual passivating behavior with time and temperature. As expected, nickel spontaneously passivates at all temperatures under study (20–80 °C). Cobalt on the other hand, is active at all temperatures but shows an active/passive-transition. Iron spontaneously passivates only at temperatures below 60 °C and activates at temperatures >60 °C. At sufficiently anodic potentials, passivity of Fe is lost by transpassive Fe dissolution to form ferrates $[FeO_4]^{2-}$. The latter is considered the most likely cause for corrosion-induced failure in alkaline batteries.

1. Introduction

Plated steel is widely used for production in alkaline battery parts (cans, covers, etc.). Low carbon steel provides structural stability at a reasonable cost. During extended shelf storage and accelerated aging tests—often carried out at elevated temperatures—low carbon steel may corrode producing soluble iron species. Presence of soluble iron species in alkaline cells undermines battery reliability. Dissolved iron might diffuse into the anode and plate on Zn particles, forming Fe dendrites that bridge anode and cathode and cause self discharge (internal cell shorting). Fig. 1 shows this dendrite formation observed in certain cases in alkaline batteries after extended storage. To prevent the formation of soluble iron, typically battery steels are coated with Ni and/or NiCo plating.

The corrosion behavior of different pure metals, such as Fe, Ni, Co, in alkaline solutions has been investigated by different research groups for several decades. In principle, in alkaline solutions iron can be dissolved as ferric (Fe(III)) or ferrate (Fe(VI)) species [1] depending on the electrode potential and temperature. Active iron dissolution in concentrated alkaline media [2–4] has been studied intensively over the years.

Transpassive iron dissolution in alkaline environment is considered less frequently. Poggendorf [5] was the first to observe the formation of ferrate(VI) species by anodic oxidation of an iron electrode in a concentrated alkaline solution. Later on, Haber [6] and Pick [7] carried out similar studies and found that a necessary condition for the formation of ferrate(VI) was pH ≥ 14. They reported that the current yield increased with electrolyte concentration (40–50% NaOH or KOH), temperature (30–70 °C), as well as with the carbon content in the iron electrode. More recently, influence of anode composition on electrochemical ferrate(VI) generation was studied by Denvir and Pletcher [8] using a three-dimensional anode. Grube and Gmelin [9] showed that the current yield for the oxidation of iron to ferrate(VI) can be increased by using direct current (dc) with a superimposed alternating current (ac) component. Other than these, several studies have been published on different reaction mechanisms for ferrate(VI) formation [10–18].

Ni and/or NiCo plating is routinely employed to protect steel from corrosion in alkaline environments. As a result, the electrochemical behavior of Ni- or Co-plated electrodes has been intensively studied. Brown et al. [19] investigated the kinetics of hydrogen evolution reaction on mild steel and Ni cathodes in concentrated NaOH solution (4–50 wt.%) in the temperature range of 15–85 °C. The behavior of Fe, Ni and Raney Ni electrodes was investigated by Ogata et al. [20] at different elevated temperatures. These authors found that Fe was seriously corroded by hot concentrated caustic whereas Ni was resistant to corrosion. More recently, the electrochemical behavior of hydroxides of Ni, Co, Mn and mixed hydroxide electrodes with well-controlled chemical composition has been studied by several research groups [21–26]. Passivity of pure nickel in alkaline electrolyte has been studied in detail by XPS

* Corresponding author. Tel.: +49 9131 852 7575; fax: +49 9131 852 7582.
E-mail address: schmuki@ww.uni-erlangen.de (P. Schmuki).

0013-4686/$ – see front matter © 2009 Elsevier Ltd. All rights reserved.
doi:10.1016/j.electacta.2009.02.022

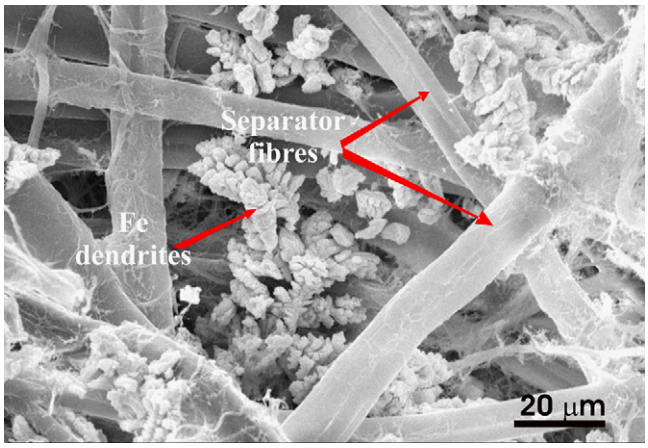

Fig. 1. SEM image of Fe dendrites formed by the deposition of dissolved Fe^{2+} growing through the separator fibers and causing internal short circuiting of a battery cell.

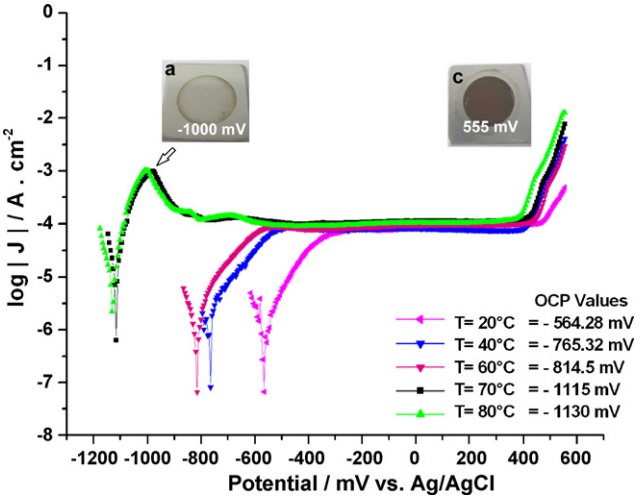

Fig. 2. Anodic polarization curves of Fe in 40% KOH solution at different temperatures.

and UPS [27] as well as with in situ X-ray scattering techniques [28]. The potential-dependence of the nature of the passive film (thickness of the film, presence of different oxidized Ni species in the layer) is directly related to oxidation/reduction events observed in polarization curves.

Compared with the large amount of work focused on the electrochemical behavior of iron and nickel in alkaline media, relatively few studies have been carried out on cobalt. Cowling and Riddiford [29] studied the anodic polarization of cobalt in sodium hydroxide solutions under potentiostatic and galvanostatic conditions. Formation and growth of passivating layer of cobaltous hydroxide were discussed based on the analysis of the current/time curves at various constant potentials. The electrochemical behavior of electroless cobalt in NaOH solution by cyclic voltammetry at different temperatures has also been investigated by Udupa and co-workers [30]. They observed the formation of different oxidized forms of cobalt (e.g., $Co(OH)_2$, CoO, Co_3O_4, and CoOOH) during electrochemical oxidation reaction. Foelske and Strehblow [31] carried out detailed surface analytical studies on passivation of cobalt in alkaline solution, demonstrating the potential-dependent thickness and chemical composition of the passive film. Novoselsky and Menlisheva [32] investigated the kinetics of initial stages of cobalt electrode passivation by voltamperometric method. They proposed the most probable adsorption mechanism and passivation model determining the kinetics of the passivation process.

In this paper, we investigate the corrosion behavior of pure metals (iron, nickel, and cobalt) in concentrated KOH (40 wt.%) at temperatures between 20 °C and 80 °C and compare it to results obtained for a NiCo-coated low carbon steel. The aim of the study is to determine critical factors and mechanisms leading to loss of passivity for these materials in alkaline solutions. In view of battery failure by internal cell shorting due to the Fe dendrite formation, we investigate the production of dissolved iron either by active or by transpassive dissolution (at various times and temperatures).

2. Experimental

Fe foil/plate of 10 mm thickness (purity ~99%), Co foil of 0.5 mm thickness (purity ~99.9%), and Ni foil/plate 10 mm thick (purity ~99%) (Advent, England) were used for electrochemical measurements. For comparison, a low carbon battery grade steel with and without a commercial NiCo coating was also studied. Electrochemical measurements were carried out in aqueous solutions of 40% KOH using a Jaissle model 1002T-NC potentiostat. Potentiodynamic polarization curves were acquired with a sweep rate of 1 mV/s. Anodic polarization curves were started at a potential 50 mV cathodic to the open circuit potential (OCP), either immediately upon immersing the working electrode sample in the solution or after waiting 20 min at the OCP. All potentials are referred to Ag/AgCl (1 M KCl) reference electrode placed in a Haber–Luggin

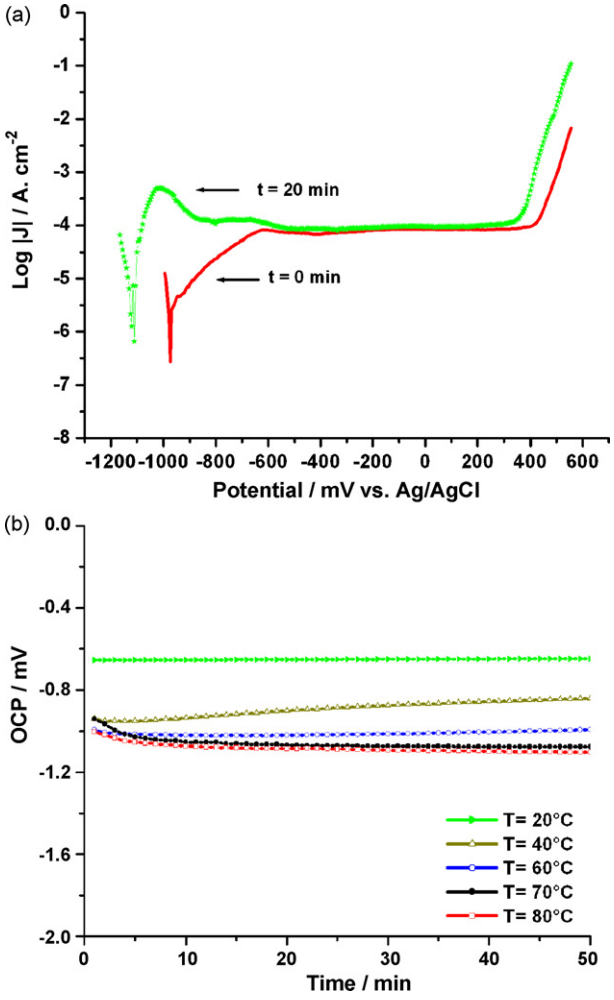

Fig. 3. Electrochemical behavior of Fe in 40% KOH—influence of temperature and time: (a) polarization curves recorded at 70 °C with and without 20 min waiting time after immersion and (b) OCP as a function of immersion time at different temperatures.

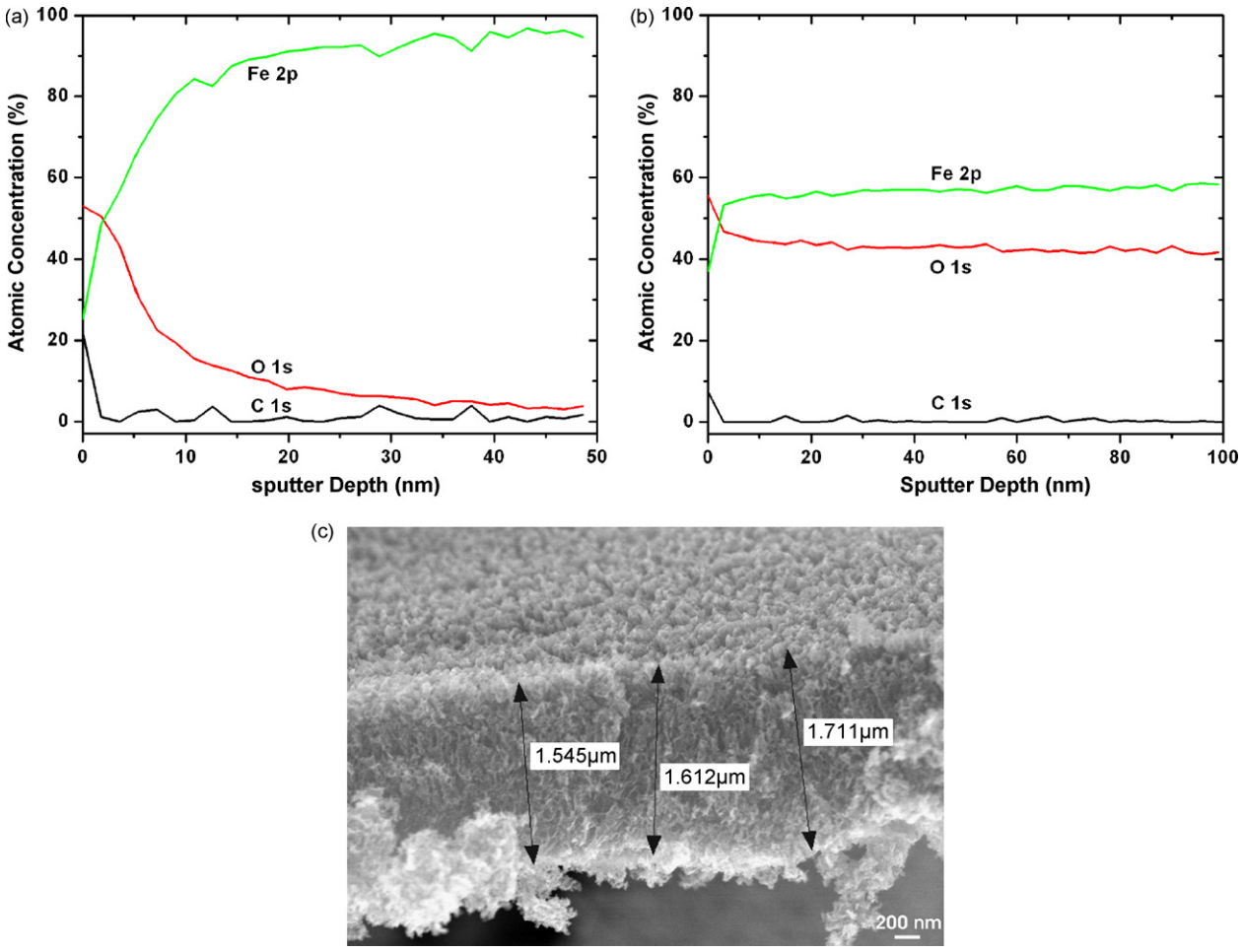

Fig. 4. (a) XPS sputter depth profile of Fe sample after polarization into the passive region; (b) XPS sputter depth profile of the Fe surface after polarization in the transpassive region; (c) SEM image of Fe surface after polarization in the transpassive region.

capillary. Temperature was maintained using a thermostat with a heating coil inserted into the electrochemical cell during measurements. Platinum foil was used as a counter electrode. All chemicals were purchased from Sigma–Aldrich, Germany.

Morphological characterization of the sample surfaces was carried out using a Scanning Electron Microscope Hitachi FE-SEM S4800. Surface composition of the samples was evaluated by means of X-ray photoelectron spectroscopy (XPS) using a PHI 5600 XPS spectrometer and Al 2 mm Kα monochromatic radiation (1486.6 eV) as the excitation source. XPS depth sputtering profile was obtained using Ar^+ ions sputtering at an accelerating energy of 3.5 kV. The vacuum pressure during measurements was less than 10^{-8} Torr. Sputtering rate of 1.8 nm/min was used. Optical images were recorded using a CCD camera.

3. Results and discussion

3.1. Electrochemical behavior of pure metals

Fig. 2 shows anodic polarization curves for Fe electrodes at different temperatures. The polarization curves were collected after 20 min at the open circuit potential (OCP). The significance of this holding time will be discussed later. From the curves in Fig. 2 it can be deduced that for temperatures of 70 °C and 80 °C, an active/passive behavior is observed while at lower temperatures an active/passive-transition is absent, i.e. the samples show a spontaneously passive behavior. Fig. 3 illustrates the influence of time on the electrochemical behavior of iron metal. At elevated temperatures, activation of Fe will take place with time as demonstrated by measuring the polarization curves either directly upon immersion of the sample into the solution, or after 20 min waiting time at the OCP. Spontaneous passivity is observed for the sample anodically polarized directly after immersion (t = 0 min in Fig. 3a). However, after 20 min in the solution the sample surface was activated, the OCP shifted in the cathodic direction, and a distinct active/passive-transition is observed in the polarization curve (t = 20 min in Fig. 3a). The activation of Fe with time is also seen in Fig. 3b, presenting the OCP values as a function of time at different temperatures. A spontaneous and fast activation is observed for temperatures >60 °C. At 20 °C and 40 °C the trend of the OCP is towards stable passivation. This temperature-induced depassivation of iron is similar to the earlier reported behavior of carbon steel in concentrated NaOH solutions at different temperatures [33].

Furthermore, at all temperatures polarization curves show a current increase at potentials >350 mV reflecting the onset of oxygen evolution and transpassive dissolution of iron as Fe^{6+} ferrate (K_2FeO_4) species. This is of high significance for alkaline battery applications as typically the battery can is coupled with the cathode MnO_2. Typical measured coupling voltages between the steel and the MnO_2 show that, the steel can easily be exposed to anodic potentials amounting to 350–450 mV vs. AgCl. Therefore, ferrate formation is a highly likely source of soluble iron. In the polarization curve of Fig. 2 the electrode surface during the experiment devel-

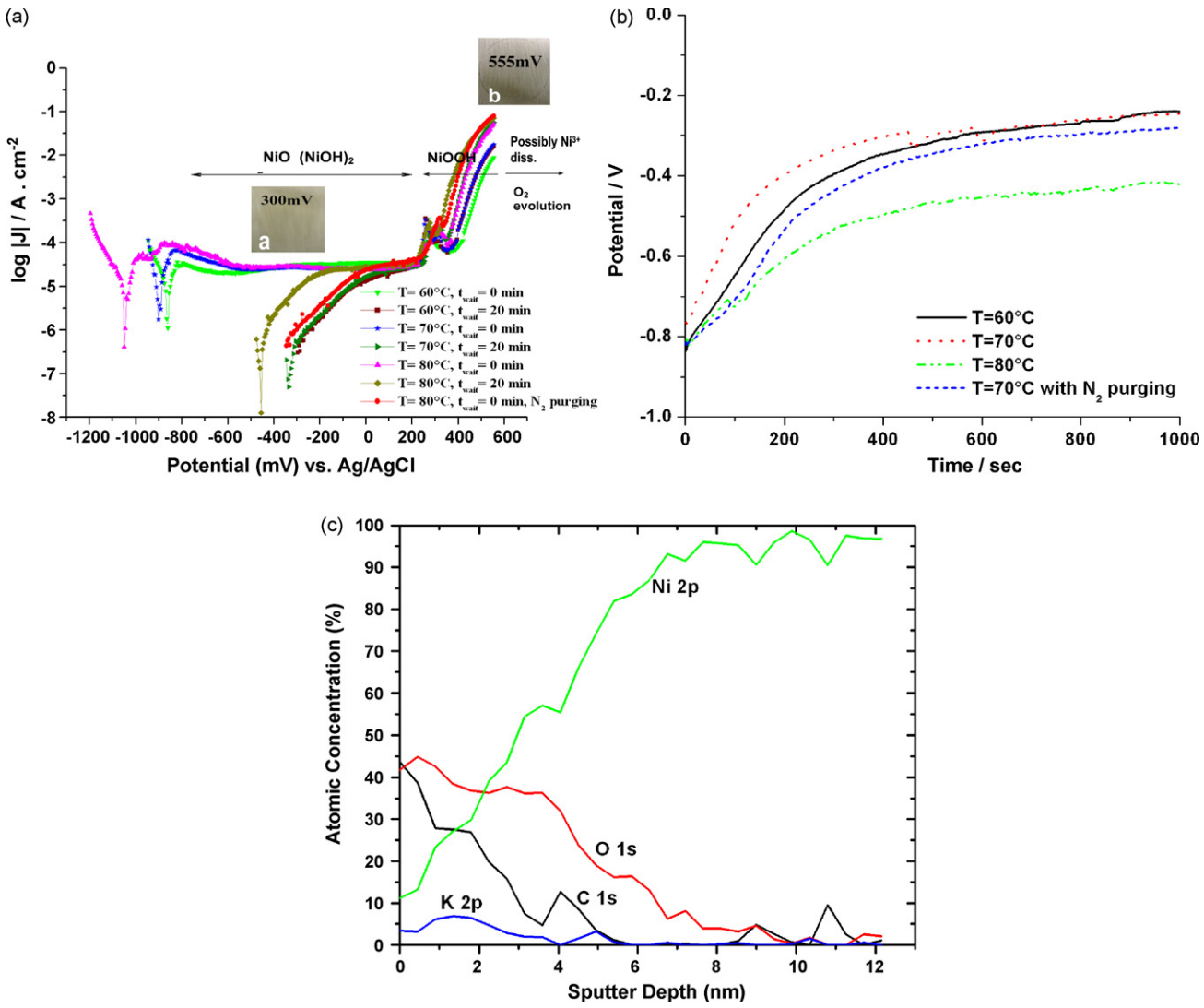

Fig. 5. (a) Polarization curves of Ni recorded at different temperatures directly after immersion in the electrolyte and after 20 min of immersion in 40% KOH; (b) Ni OCP in 40% KOH as a function of immersion time at different temperatures; (c) XPS sputter depth profile of the Ni surface after polarization into the transpassive region.

ops a purplish color in this potential region, indicative of the ferrate formation. This finding is in agreement with observation of ferrate formation in concentrated alkaline solutions reported in the literature [11,13–18,34]. After removal of the Fe sample, as shown in the insets of Fig. 2, a thick porous oxide film is formed on the substrate. The nature of the corrosion product on the iron electrode surface was studied by XPS and SEM. Fig. 4a and b shows XPS depth profiles of the corrosion film formed upon sample polarization in the passive range, as well as after polarization in the transpassive region, respectively. The thickness of the passive film is ~5 nm; however, polarization in the transpassive region leads to a strong thickening of the oxide layer, with a thickness exceeding 1 μm. Fig. 4c shows an SEM image of the surface layer formed in the transpassive region indicating presence of a porous film with a thickness of 1.5 μm.

In order to explain the transpassive behavior one may consider both the oxidation reactions of metallic iron and Fe^{3+} (Fe_2O_3) species to ferrate as listed below [3]:

$$Fe^{3+} + 4H_2O \leftrightarrow FeO_4^{2-} + 8H^+ + 3e^-, \qquad \varepsilon_o = +1.9\,V$$

$$Fe + 4H_2O \leftrightarrow FeO_4^{2-} + 8H^+ + 6e^-, \qquad \varepsilon_o = +1.2\,V$$

Ferrate FeO_4^{2-} may undergo disproportionation to Fe_3O_4 or Fe_2O_3:

$$FeO_4^{2-} \rightarrow Fe^{3+} + O_2$$

$$2FeO_4^{2-} + 10H^+ \rightarrow 2Fe^{3+} + 1.5O_2 + 5H_2O$$

The Fe^{3+} species will further react with hydroxyl ions OH^- and precipitate as $Fe(OH)_3$ or dehydrate to Fe_2O_3 detected on the low carbon steel surface under alkaline battery conditions (results not shown). The transpassive dissolution of Fe as ferrate and the follow-up reactions hence explain the presence of the thick, porous surface layers after polarization in the transpassive region.

The electrochemical behavior of nickel at different temperatures is shown in Fig. 5a and b. Nickel displays a distinctly different behavior compared to metallic iron. Passivation of nickel electrode surface with time takes place at all temperatures, clearly indicated by the OCP values recorded as a function of time (Fig. 5b). The polarization curves show spontaneous passivity at all temperatures after 20 min immersion time at the OCP. Anodic polarization directly upon immersion in the concentrated KOH solution shows a slightly pronounced active/passive-transition due to formation of Ni(II) oxide/hydroxide layer (region (a) in Fig. 5a) described in

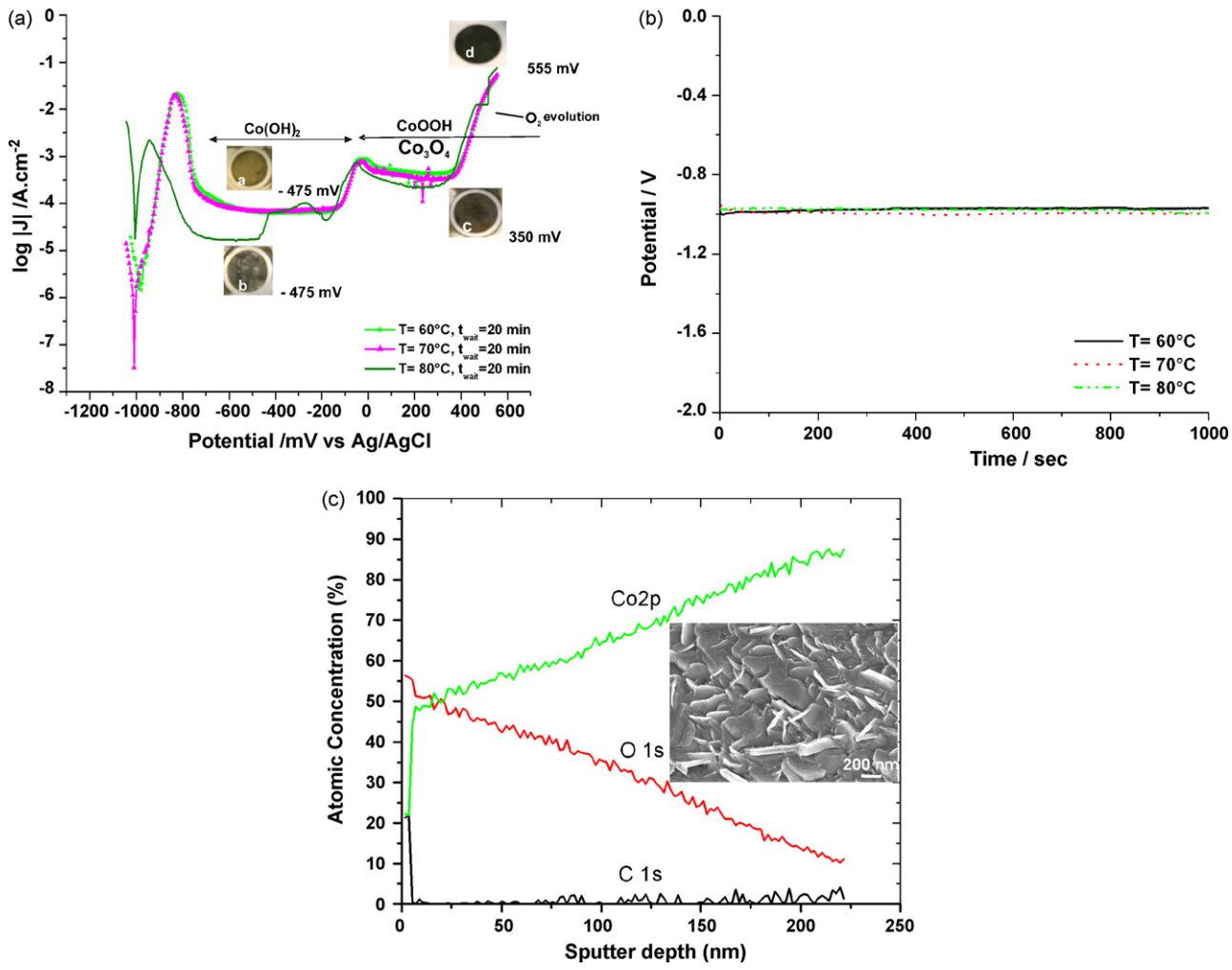

Fig. 6. (a) Polarization curves of Co recorded at different temperatures directly after immersion in the electrolyte and after 20 min of immersion in 40% KOH; (b) Co OCP in 40% KOH as a function of immersion time at different temperatures; (c) XPS sputter depth profile of the Co surface after polarization into the transpassive region.

the literature (e.g., [27,28,35]). Onset of high currents at more positive potentials corresponds to formation of nickel oxyhydroxide, NiOOH, along with oxygen evolution [20]. Transpassive dissolution may take place at higher potentials, as discussed in the literature [36,23]. In the transpassive region, only a thin layer of Ni oxide is present on the electrode surface as confirmed by XPS analysis shown in Fig. 5c.

The anodic polarization behavior of cobalt is illustrated in Fig. 6a. It is noteworthy that at all temperatures (60 °C, 70 °C, and 80 °C) and independent of time in the KOH electrolyte, cobalt displays a prominent active–passive peak corresponding to cobalt metal oxidation to Co^{2+} species and subsequent formation of $Co(OH)_2$ passive layer [29,31]. The OCP potential measured as a function of time (Fig. 6b) also indicates that the surface is active at these temperatures. Upon anodic polarization to more positive potentials, Co^{2+} is further oxidized to Co^{3+} and the passive layer consists of CoOOH and/or Co_3O_4 [30–32]. At potentials >350 mV oxygen evolution leads to current increase. The optical micrographs of the electrode surface (insets a–d) collected at different ranges of polarization curve show a presence of thick corrosion layers on the surface. An XPS depth profile analysis of the surface layer formed at 350 mV and the corresponding SEM image show formation of ~150–250 nm thick oxide film with a rough surface appearance (Fig. 6c). At higher potentials the high resolution O 1s signal (not shown here) indicates the presence of OOH^- on the surface, suggesting formation of cobalt oxyhydroxide.

In brief, distinct differences in the electrochemical behavior of pure Fe, Ni and Co in 40% KOH can be observed. Iron spontaneously passivates at temperatures below 60 °C and activates at $t > 60$ °C, showing an active/passive-transition upon anodic polarization. At higher anodic potentials, transpassive dissolution by formation of ferrate species is observed. Nickel spontaneously passivates at all temperatures studied (20–80 °C). Cobalt, on the other hand, is active at all investigated temperatures (20–80 °C) but can be passivated upon anodic polarization.

3.2. Electrochemical behavior of unplated and plated carbon steel

Fig. 7a illustrates the electrochemical behavior of the uncoated low carbon steel substrate at different temperatures. Spontaneous passivity is observed at lower temperatures between 20 °C (not shown), 60 °C and 70 °C (Fig. 7a), but active dissolution followed by passivation takes place at 80 °C, similar to behavior of pure iron. Fig. 7b shows the polarization curves of the NiCo plated (coated) steel. When the polarization is started immediately after immersion in the electrolyte solution, an active/passive-transition is observed at all temperatures. This behavior is similar to pure Co. After 20 min waiting at the OCP, spontaneous passivation of the surface may take place. In this case, the coating is significantly anodic with respect to the uncoated steel substrate. The behavior of the coated steel under anodic potential reflects the presence of both cobalt and nickel on the surface as the oxidation peaks at more positive potentials can

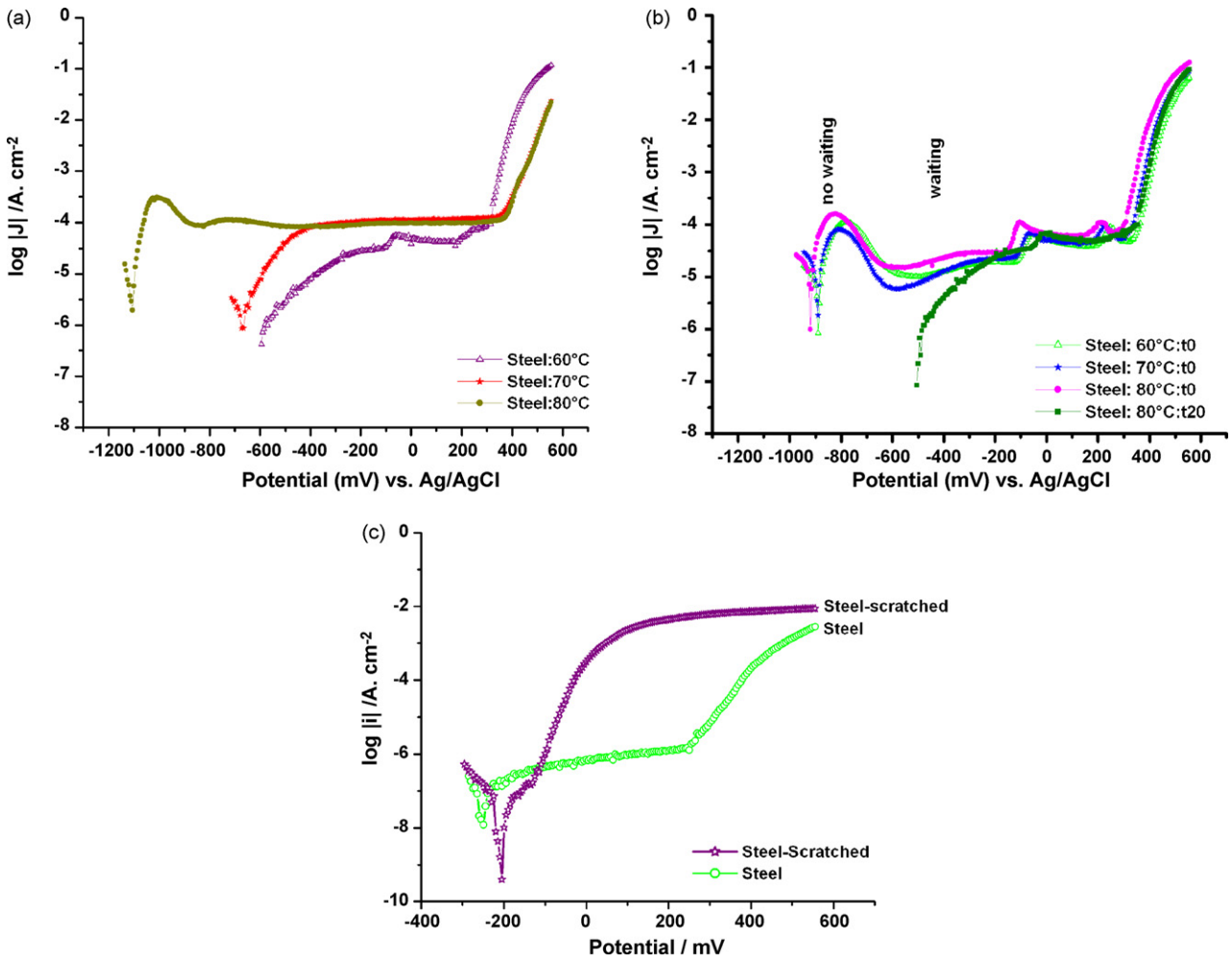

Fig. 7. (a) Polarization curves of low carbon unplated steel at different temperatures; (b) polarization curves of plated steel at different temperatures collected with (t = 20 min) and without waiting time (t = 0) in electrolyte solution; (c) polarization curves of intact and scratched plated steel in 0.2 M NaCl in borate buffer (pH 8.3).

be attributed to different cobalt and nickel oxidation reactions (see Figs. 5a and 6a).

Effect of presence of defects in the coating was investigated by scratching the plated steels and then polarizing the sample in 0.2 M NaCl solution. Plating on the steel surface was damaged by scratching with a diamond pen. EDX mapping of the surface confirmed removal of protective plating layer and exposure of steel substrate. Polarization curves of intact and scratched steel samples (Fig. 7c) show that presence of defects in the plating significantly enhances onset of localized corrosion, with a significantly lower pitting potential observed for the scratched sample.

As the electrochemical behavior of the pure metals, the low carbon steel, and the NiCo coating are strongly temperature-dependent, it should be considered that accelerated testing under elevated temperatures may not reflect the failure modes at lower temperatures. The findings indicate that failure of the coated steel is possible due to the active dissolution of the steel substrate at defects of the coating (corresponding to the behavior of pure iron). Moreover, accelerated dissolution of steel could take place at higher anodic potentials due to transpassive dissolution of iron.

4. Conclusions

- Presence of soluble iron species undermines battery reliability by causing internal cell shorting and/or gassing (leakage). Behavior of pure metallic iron, nickel and cobalt in concentrated alkaline solutions sheds light on corrosion of plated battery steel materials. In 40% KOH, pure Fe spontaneously passivates at temperatures below 60 °C; and activates at temperatures >60 °C. The surface of nickel spontaneously passivates at all temperatures under study (20–80 °C) and should not contribute to production of soluble species. Cobalt shows an active/passive-transition at all investigated temperatures (20–80 °C).
- NiCo plated battery steel shows a time-dependent electrochemical behavior, reflecting the presence of both nickel and cobalt in the coating. Defects in the coating enhance the danger of generation of soluble corrosion production by dissolution of the steel substrate.
- Soluble iron may be generated from active and/or transpassive dissolution of steel. Depassivation of iron occurs at temperatures over 60 °C. Therefore, accelerated testing at elevated temperatures may lead to erroneous conclusions on possible failure modes of coated steels.
- If an exposed iron surface is created on a plated steel of a MnO_2/Zn battery, the most likely Fe dissolution mechanism is transpassive dissolution, as the coupling with MnO_2 on the battery wall polarizes the surface into the range of possible ferrate formation.

Acknowledgements

The authors are grateful to Dr. Jan Macak for helping in electrochemical experiments and Dr. Helga Hildebrand for XPS analysis.

References

[1] I. Serebrennikova, IR 07-06, Electrochemical Fundamentals of Can Steel Corrosion in Alkaline Batteries, 2007.
[2] R.D. Armstrong, I. Baurhoo, J. Electroanal. Chem. 40 (1972) 325.
[3] D.D. MacDonald, B. Roberts, Electrochim. Acta 23 (1978) 781.
[4] H. Zhang, S.-M. Park, J. Electrochem. Soc. 141 (1994) 718.
[5] J.C. Poggendorf, Pogg. Ann. 54 (1841) 161.
[6] F. Haber, Z. Elektrochem. 7 (1900) 215.
[7] W. Pick, Z. Elektrohcem. 7 (1901) 713.
[8] A. Denvir, D. Pletcher, J. Appl. Electrochem. 26 (1996) 823.
[9] G. Grube, H. Gmelin, Z. Elektrochem. 26 (1920) 153.
[10] J. Tousek, Collect. Czech. Chem. Commun. 27 (1962) 914.
[11] F. Beck, R. Kaus, M. Oberst, Electrochim. Acta 30 (1985) 173.
[12] K. Bouzek, I. Rousar, J. Appl. Electrochem. 23 (1993) 1317.
[13] A.S. Venkatadri, H.H. Bauer, W.F. Wagner, J. Electrochem. Soc. 121 (1974) 249.
[14] K. Bouzek, M. Lipovska, M. Schmidt, I. Rousar, A.A. Wragg, Electrochim. Acta 44 (1998) 547.
[15] K. Bouzek, I. Rousar, H. Bergmann, K. Hertwig, J. Electroanal Chem. 425 (1997) 125.
[16] K. Bouzek, L. Flower, I. Rousï Ar, A.A. Wragg, J. Appl. Electrochem. 29 (1999) 569.
[17] M. De Koninck, T. Brousse, D. Bélanger, Electrochim. Acta 48 (2003) 1425.
[18] M. De Koninck, T. Brousse, D. Bélanger, Electrochim. Acta 48 (2003) 1435.
[19] A.P. Brown, M. Krumpelt, R.O. Loutfy, N.P. Yao, J. Electrochem. Soc. 129 (1982) 2481.
[20] Y. Ogata, H. Hori, M. Yasuda, F. Hine, J. Electrochem. Soc. 135 (1988) 76.
[21] A. Audemer, A. Delahaye, R. Farhi, N. Sac-Epee, J.-M. Tarascon, J. Electrochem. Soc. 144 (1997) 2614.
[22] D. Belanger, G. Laperriere, J. Electrochem. Soc. 137 (1990) 2355.
[23] M.A. Hopper, J.L. Ord, J. Electrochem. Soc. 120 (1973) 183.
[24] D.H. Fritts, J. Electrochem. Soc. 129 (1982) 118.
[25] A.E. Bohe, J.R. Vilche, A.J. Arvia, Corros. Sci. 34 (1993) 151.
[26] V. Srinivasan, J.W. Weidner, J. Newman, J. Electrochem. Soc. 148 (2001) A969.
[27] H.-W. Hoppe, H.-H. Strehblow, Surf. Interf. Anal. 14 (1989) 121.
[28] S.L. Medway, C.A. Lucas, A. Kowal, R.J. Nichols, D. Johnson, J. Electroanal. Chem. 587 (2006) 172.
[29] R.D. Cowling, A.C. Riddiford, Electrochim. Acta 14 (1969) 981.
[30] T.R. Jayaraman, V.K. Venkatesan, H.V.K. Udupa, Electrochim. Acta 20 (1975) 209.
[31] A. Foelske, H.-H. Strehblow, Surf. Interf. Anal. 34 (2002) 125–129.
[32] I.M. Novoselsky, N.R. Menglisheva, Electrochim. Acta 29 (1984) 21.
[33] J.-Y. Zou, D.-T. Chin, Electrochim. Acta 33 (1988) 477.
[34] K. Bouzek, H. Bergmann, Corros. Sci. 41 (1999) 2113.
[35] P.-H. Lo, W.-T. Tsai, J.-T. Lee, M.P. Hung, J. Electrochem. Soc. 142 (1995) 91.
[36] J.L. Ord, J.C. Clayton, D.J. DeSmet, J. Electrochem. Soc. 124 (1977) 1714.